Research Square

Preprints are preliminary reports that have not undergone peer review.
They should not be considered conclusive, used to inform clinical practice,
or referenced by the media as validated information.

A gravity-based framework for the spatial allocation and distribution of storage capacity to facilitate reuse of construction and demolition waste

Ling Min Tan

lingmin.tan@sheffield.ac.uk

The University of Sheffield

Hadi Arbabi

The University of Sheffield

Research Article

Keywords:

Posted Date: November 25th, 2026

DOI: https://doi.org/10.21203/rs.3.rs-11727670/v1

License: This work is licensed under a Creative Commons Attribution 4.0 International License.
Read Full License

Additional Declarations: No competing interests reported.

A gravity-based framework for the spatial allocation and distribution of storage capacity to facilitate reuse of construction and demolition waste

Ling Min Tan[1,*] and Hadi Arbabi[1]

[1]School of Mechanical, Aerospace and Civil Engineering, The University of Sheffield, Sheffield S1 3JD, UK.

[*]Corresponding author: lingmin.tan@sheffield.ac.uk

Abstract

This study examines how the location and capacity of intermediary storage hubs affect reuse of construction and demolition waste in the built environment. A gravity-based framework is developed to investigate how varying number, location, and size of storage capacities affect material flows across a hypothetical network under various constraint conditions. Travel deterrence is applied to the model, presented in a case study of Great Britain's road-transport network, to study the impacts of distance cut-off thresholds on material flows and the effects of the spatial distribution of storage capacity scaled by supply, demand and node centrality. The results show that under flow-constrained conditions in a homogeneous network, maximum reuse is achieved by maximising recovery efficiency when supply is limited. The study also investigates spatial allocation of storage infrastructure when total capacity is fixed, then determines the spatial agglomeration of more centralised or distributed storage network under different material and transport limitations.

Keywords: Built environment, circular economy, material reuse, spatial logistics, gravity model

1 Introduction

The construction and demolition sector generates an estimated 2.2 billion tonnes of waste annually, representing roughly one-third of global waste streams [1]. Construction and demolition waste (CDW) is typically defined as solid materials such as building debris, rubble, concrete, steel, bricks and timber arising from the construction, renovation and demolition of buildings, infrastructure or roads [2]. On local scale, CDW makes up a significant portion of the total solid waste stream in municipal areas, especially in developing countries where there is high demand for large infrastructure and housing provision to meet the increasing populations in urbanised areas [3, 4].

In recent years, the adoption of circular construction practices in CDW management has gained increasing importance, with regulations in many countries now mandating such approaches to improve resource efficiency and reduce environmental impacts [5, 6]. The overarching aim of the circular economy (CE) framework is to extend material lifecycles through repair, refurbish, reuse and recycling strategies. While priority is given to retaining buildings in use for as long as possible, when building demolition or deconstruction is inevitable as the building no longer fit for its purpose or service as a whole, the components can still be recovered and reused [7].

To improve circularity in the built environment, substantial efforts have been made in the building sector to develop CDW recovery techniques and facilities globally, as demonstrated by a growing number of literature review articles on CDW management [8–11]. Among these, tools such as Building Information Modeling [12], IoT-enabled smart tracking systems [13] and Life Cycle Assessments [14] have been widely applied to improve material recovery rates for optimising resource efficiency of the built environment and hence, reducing their overall embodied carbon emission. In a CE context, promoting direct reuse of these CDW materials is essential to drive embodied carbon emissions low. However, reuse rates are consistently lower than recycling rates, despite high CDW recovery rates reported [15]. The reported rates of CDW recovery, which may vary by countries and material types, are largely driven by downcycling of waste material into recycled aggregated products rather than high-value direct reuse. For example, in the UK, about 96% of the structural steel is recovered from waste but only 5% of the materials is directly reused [16]. Similarly, in the EU, although the overall recovery of CDW is reported at around 90% under the Waste Framework Directive, only 1% of the recovered elements are effectively reused in construction and majority of the mineral fractions such as concrete and brick are converted to recycled aggregates [17, 18].

The concept of reverse logistics, defined as 'return of post-sale and post-consumption goods to the productive cycle through reverse distribution channels' [19], or simply the process of redirecting secondary materials to new uses, is instrumental for component-level circularity [20]. Integration of CDW in reverse logistics supply chains (RLSC) has gained growing attention as an enabler for extending product lifetimes by coordinating availability of storage facilities, optimising operational costs associated with on-site material sorting, inspection and maintenance, and also minimising transport-related emissions when it comes to shipping bulk masses and volumes [21, 22]. In the context of CDW reuse, existing literature suggests that even where technical feasibility for component-level reuse is improving with advancing building designs and implementation of smart technologies and circular practices in building construction and demolition. These include the adoption of material passports and smart material flow tracking systems. However, in closed-loop supply chain analysis, storage and logistics are often identified as critical barriers to the reuse of CDW [23]. The absence of dedicated storage points means that reuse flows remain highly fragmented and opportunistic when matching supply and demand for specific materials [24]. In the literature, these facilities are variously described as storage hubs, circular construction hubs or waste transfer stations and function as material and component banks connecting demolition-side supply to construction-side demand [25, 26]. While some emerging frameworks for digital material banks and business models offer ways of integrating storage capabilities and connecting demolition sites, storage hubs and new construction projects through logistic networks, these remain largely at the exploratory stage and are not yet embedded in mainstream practices [27, 28].

To summarise, reuse of CDW is widely recognised as a high-value CE strategy, but current studies show their reuse rates remain marginal due to a combination of technical, economic and operational barriers across the supply chain. Overall, the literature suggests that overcoming storage and logistical barriers will require coordinated investments in physical infrastructure to justify the additional costs and risks associated with managing reusable materials across space and time [28, 29]. This emphasises the need to develop an appropriate approach to establish an inter-connected system of storage infrastructure networks, coordinating the supply and demand across the circular construction value chain, for widespread component reuse. Furthermore, the feasibility of storage networks for CDW

reuse should be examined at a system-level to better understand the amount of space required and their spatial distribution in order to justify resource savings and the transport-related emissions [25]. In fact, the roles of centrally-managed storage points for managing CDW are, to some extents, institutionally recognised in emerging policy instruments such as the Extended Producer Responsibility initiatives [30], and yet this topic remains under-researched and poorly understood with very little research evidence with limited scholarly contributions beyond the literature of RLSC that primarily focusing on recycling [31].

The aim of this study is to investigate the key questions on how much storage space is needed, and where should it be located? From a system-level perspective, this paper seeks to examine how the location and capacity of storage facilities affect circulation of CDW materials and the overall carbon emissions. This allows us to understand how such facilities enable the redirection of materials supplied from demolition sites to a temporary storage through the transport network, and subsequently resupplied to new construction sites for reuse while minimising waste disposal and the need for primary resource extraction. The rest of this paper is organised as follows. The next section provides a brief overview of the modelling approach and the formal analytical formulation of the storage network model. This is followed by the results section to discuss the key findings, including a case study of Great Britain to present as a potential application of the method in the real world. The final section concludes the study with a summary of the key contributions of this work and outlines the areas for future research work.

2 Materials and Methods

2.1 Conceptual framework

This section outlines the development of a novel network model for capturing additions and removals of materials from the existing building stock through construction and demolition activities, which represent the supply and demand of such resources respectively, as illustrated in Figure 1. These form a hybrid supply- and demand-driven model for tracking flows between the nodes, where each node represents a geographical-bounded area (e.g., city, district, region or country) that can simultaneously have demolition-supply, construction-demand and storage capacity. The role of storage points in the framework can be interpreted as a physical space for holding up reusable CDW material temporarily before a demand for the specific material arises, or space becomes available, at a new construction site to form a closed-loop system. Direct supply from demolition and construction is excluded as this may not be seen as a storage problem and the flow is allocated before considering sending the material to a temporary storage.

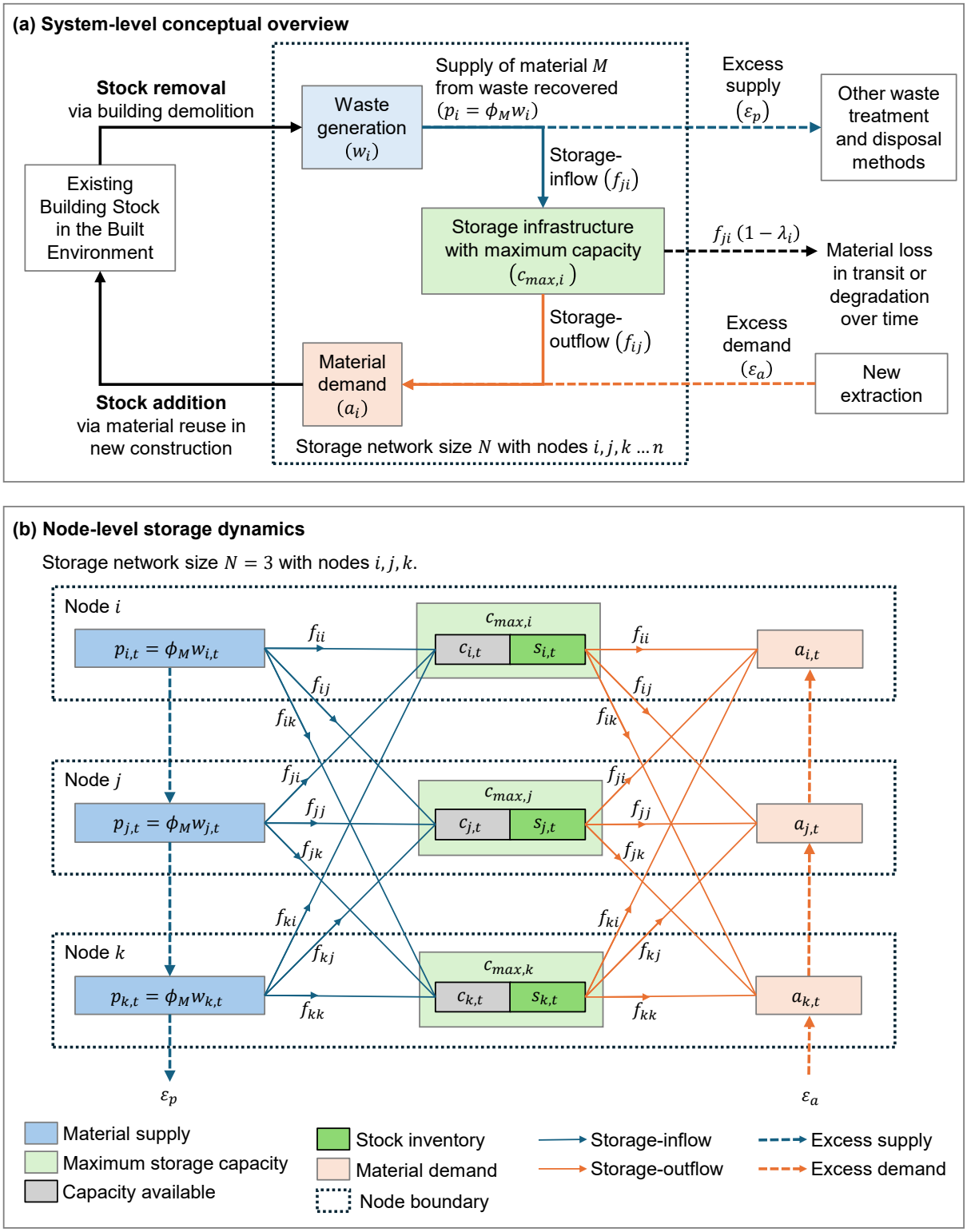


Figure 1: **(a)** System-level conceptual overview of the framework showing the dynamic flow interactions between the storage network internal variables within the boundary (e.g., Waste generation, storage and demand) and the external environment(e.g., existing building stock, waste disposal and new extraction) to estimate excess supply and excess demand. **(b)** Node-level network representation with interconnected nodes and edges, illustrating material flows and storage dynamics including storage inflows to fill spaces available and storage outflows to meet a demand.

The purpose of this model is to simulate the dynamic flows of CDW material, distributed through a group of storage points in an interconnected network, overlaying with transport links. This means that the edges between the nodes are weighted on the basis of the amount of material transported and their travel distances. The flows can be broken down into two directions: storage-inflow and storage-outflow to form a closed-loop system. Storage-inflow refers to supply of materials from a demolition site to fill up a storage whereas storage-outflow refers to withdrawal of materials from a storage to meet a demand at a new construction site. The constraints applied are the fixed supply and demand of materials by how much construction and demolition works are taking place within a fixed spatial boundary, and also the limited storage capacity. In the storage-inflow direction, excess supply (ε_p) can be calculated as the remaining materials redirected to disposal when there is no sufficient storage space available across the whole network, whereas in the storage-outflow direction, excess demand (ε_a) is the measure of how much virgin materials from new extraction is needed when there is insufficient stock material across all the storage points to meet the demand.

For the mathematical expression of the storage network model, the availability of supply, demand and the maximum storage capacity available within their respective boundaries of a node, i, at a time t, can be denoted as $a_{i,t}$, $p_{i,t}$ and c_{max_i} respectively. For dynamic flows, the time interval, Δt, equals the time taken to accumulate the materials required for meeting the respective supply and demand at each location.

To provide a comprehensive model of CDW reuse flows, two efficiency factors are introduced. Firstly, ϕ_M as the material yield factor of a specific material type M, to indicate how much reusable materials are reclaimed from the waste streams w_i at any node, therefore, the supply of material M at time t can be expressed as:

$$p_{i,t} = \phi_M w_{i,t} \tag{1}$$

The second factor is λ_i, which represents the retention factor at storage node i. It captures material losses during transit and degradation over time. Specifically, λ_i reduces the amount of material carried over from one timestep to the next, acting as a penalty on long-term storage. As a result, the longer material remains in storage, the lower its effective retention.

Putting these elements together provides a way to assess the benefits of the storage network, where the amount of material stock received at each storage point can be interpreted as savings from demolition by diverting material away from alternative disposal routes, such as recycling into aggregates or landfilling. On a system-level, considering all inflows and outflows at every node of the network, material-throughput as a product of material mass and the distance travelled, excess demand, excess supply can also be quantified, as illustrated in Figure 1.

2.2 Analytical formulation of a gravity-based spatial interaction model

This section presents the derivation of the analytical formulations that describe the conceptual framework as a generic network model for analysing material flows into and out of storage, accounting for losses in transit and material degradation. A gravity-based model is used to predict spatial interactions between a set of origins and destinations based on their supplying or receiving potentials. The potentials of the nodes are related to their sizes and locations, as interactions between two nodes tend to weaken as the distance between them increases [32]. This is also known as the distance-decay effect [33]. In multidisciplinary research, there have been variations in the development and application

of gravity-based models, for example, the gravity model of trades in economics to analyse market potentials [34], and the gravity model of migration in urban geography to predict population growth [35].

Building on the concept of gravity-based models, the General Theory of Movement provides a mathematical interpretation for describing spatial interactions across a network of varying supplying or receiving potentials across the nodes [36]. For a network of size N with nodes $i, j, k, ..., n$, the quantity of material flowing from node i to node j can be modelled as:

$$f_{ij} = \alpha_i^{1-a} O_i \beta_j^{1-b} D_j l_{ij}, \tag{2}$$

where O_i and D_j represent the overall availability of supply at origin i and the overall receiving capacity at destination j, respectively. The terms α_i and β_j are proportionality factors that balance total mass flows across the network, and l_{ij} is an accessibility function between nodes i and j. The exponents a and b determine the constraint conditions, as demonstrated in the next section.

The proportionality factors are defined as:

$$\alpha_i = \left(\sum_{j=1}^{N} \beta_j^{1-b} D_j l_{ij} \right)^{-1} \tag{3}$$

$$\beta_j = \left(\sum_{i=1}^{N} \alpha_i^{1-a} \, O_i l_{ij} \right)^{-1} \tag{4}$$

The accessibility function l_{ij} is a decreasing function over increasing distance or travel cost, as a measure of the ease of material movement between nodes. In this study, l_{ij} is specified below using a power-law distance-decay function:

$$l_{ij} = {d_{ij}}^{-\theta} \tag{5}$$

where d_{ij} is the pairwise origin-destination distance between nodes i and j, and $\theta \geq 0$ is the distance-decay parameter. Larger values of θ impose a stronger penalty on longer journeys, thereby representing travel deterrence and reducing the likelihood of travelling long distances.

2.2.1 Constraint conditions and storage dynamics

For the purpose of this study, a more flexible constraint formulation is adopted to alternate between origin-constrained and destination-constrained conditions, depending on the relative magnitudes of the total supplying potentials from origins and the total receiving capacities at destinations [37]. The parameters a and b are set to zero or one to specify the constraint condition as follows.

Origin-constrained model ($a = 1$, $b = 0$) applies when total supply is less than or equal to total receiving capacity, $\sum_i O_i \leq \sum_j D_j$, As all supply is allocated, and flows are constrained by origin availability. Under this condition, Eq. 2 can be simplified to:

$$f_{ij} = \alpha_i O_i \, D_j l_{ij} \tag{6}$$

Destination-constrained model ($a = 0$, $b = 1$) applies when total receiving capacity is less than to-

tal supply, $\sum_j D_j < \sum_i O_i$. As all receiving capacity is filled, and flows are constrained by destination capacity. Under this condition, Eq. 2 can be simplified to:

$$f_{ij} = \beta_j O_i \, D_j l_{ij} \tag{7}$$

Substituting the proportionality factors from Eq. 3 and 4 yields the following expressions for total inflows and outflows. For the origin-constrained condition, replacing α_i in Eq. 6 gives:

$$\sum_{i=1}^{N} f_{ij} = D_j \sum_{i=1}^{N} \frac{O_i l_{ij}}{\sum_{k=1}^{N} D_k l_{ik}} \tag{8}$$

$$\sum_{j=1}^{N} f_{ij} = O_i \tag{9}$$

For the destination-constrained case, replacing β_j in Eq. 7 gives:

$$\sum_{i=1}^{N} f_{ij} = D_j \tag{10}$$

$$\sum_{j=1}^{N} f_{ij} = O_i \sum_{j=1}^{N} \frac{D_j l_{ij}}{\sum_{k=1}^{N} O_k l_{kj}} \tag{11}$$

The net flow at node i is the difference between total inflows received from all other nodes and total outflows withdrawn to all other nodes within the same time period. Storage levels at an individual storage point i at time t, denoted $s_{i,t}$, can be obtained by summing the existing stock carried forward from previous time, $t-1$, adjusted by a retention factor $\lambda_i \in [0, 1]$, and the net flows, as shown below:

$$s_{i,t} = \lambda_i s_{i,t-1} + \sum_{j=1}^{N} f_{ji,t} - \sum_{j=1}^{N} f_{ij,t} \tag{12}$$

2.2.2 Storage-inflow constraints

For storage-inflow, the constraint condition is determined by the availability of supply material from waste at origins ($p_{j,t}$) and the receiving capacity at destination storage points ($c_{i,t}$):

Supply-constrained condition. When the total supply is less than or equal to the total available storage capacity, $\sum_j p_{j,t} \leq \sum_i c_{i,t}$, all supply is allocated based on the capacity and accessibility of the storage available. The total inflow to node i can be modelled as:

$$\sum_{j=1}^{N} f_{ji,t} = c_{i,t} \sum_{j=1}^{N} \frac{p_{j,t} {d_{ij}}^{-\theta}}{\sum_{k=1}^{N} c_{k,t} {d_{kj}}^{-\theta}} \tag{13}$$

Capacity-constrained condition. When the total supply exceeds the total available storage capacity, $\sum_j p_{j,t} > \sum_i c_{i,t}$, inflows are limited by the remaining storage capacity. The total inflow to node

i can be modelled as:

$$\sum_{j=1}^{N} f_{ji,t} = c_{i,t} = c_{\max,i} - \lambda_i s_{i,t-1} \tag{14}$$

where $c_{\max,i}$ is the maximum storage capacity at node i. Excess supply ($\varepsilon_{p,t}$) due to insufficient storage space can be calculated as:

$$\varepsilon_{p,t} = \sum_{j=1}^{N} p_{j,t} - \sum_{i=1}^{N} (c_{\max,i} - \lambda_i s_{i,t-1}) \tag{15}$$

2.2.3 Storage-outflow constraints

For storage-outflow, two scenarios are considered based on the relationship between available stored material and total demand ($a_{j,t}$):

Demand-constrained condition. When total stored material exceeds the total demand, $\sum_i \lambda_i s_{i,t-1} > \sum_j a_{j,t}$, only a portion of stored material is withdrawn, distributed according to accessibility. The total outflow from node i can be modelled as:

$$\sum_{j=1}^{N} f_{ij,t} = \lambda_i s_{i,t-1} \sum_{j=1}^{N} \frac{a_{j,t} {d_{ij}}^{-\theta}}{\sum_{k=1}^{N} \lambda_k s_{k,t-1} {d_{kj}}^{-\theta}} \tag{16}$$

Stock-constrained condition. When available stored material is less than or equal to the total demand, $\sum_i \lambda_i s_{i,t-1} \leq \sum_j a_{j,t}$, all stored material is withdrawn, the total outflow from node i can be modelled as:

$$\sum_{j=1}^{N} f_{ij,t} = \lambda_i s_{i,t-1}. \tag{17}$$

Excess demand ($\varepsilon_{a,t}$) due to insufficient stored material, causing new extraction to meet this demand, can be calculated as:

$$\varepsilon_{a,t} = \max \left[0, \sum_{j=1}^{N} a_{j,t} - \sum_{i=1}^{N} \lambda_i \, s_{i,t-1} \right]. \tag{18}$$

2.3 Travel deterrence

Spatial constraints can be implemented in the model as travel deterrence, which represents the cost of the journey between two nodes based on the locations and accessibility of the storage sites.

2.3.1 Carbon intensity and transport emissions

Travel deterrence is incorporated in the formulations through the distance-decay parameter θ in the accessibility function, shown in Eq. 5, which can be interpreted as a mechanism for penalising the increasing economic, operational, or environmental cost of longer journeys. Transport-related carbon emissions can be evaluated as the associated environmental impact increases with material weight transported and distance travelled. Let e denotes the carbon intensity of transport per unit mass per unit distance, which is usually expressed in terms of CO_2e per km-tonne, then the total transport

emissions, E, for the network can be estimated as:

$$E = e \sum_{i=1}^{N} \sum_{j=1}^{N} f_{ij} d_{ij}, \tag{19}$$

where f_{ij} is the material flow from nodes i to j, and d_{ij} is the corresponding travel distance. Therefore, by varying θ and e, the model explores how travel deterrence and carbon intensity affect the material flow distribution and storage utilisation.

2.3.2 Network spatial characteristics

The spatial distribution of storage sites determines the pattern of travel distances and the accessibility of nodes. To investigate the impact of spatial distribution on material flows, the model is evaluated under a range of scenarios that vary key spatial characteristics of the network. These include the network size, N, defined as the total number of storage sites, as well as network topology, which refers to the spatial arrangement of sites and influences the average travel distances and the distribution of node centrality. Considering directional travel distances to capture asymmetries that may arise from network structure, one-way routes, or transport mode constraints, pairwise distances between nodes, d_{ij}, are represented in the form of a network adjacency matrix, $[d_{ij}]$. In this case, the self-loop distance for intra-flows within the boundary of the same node is calculated as

$$d_{ii} = \frac{128}{45\pi} d_{min} \tag{20}$$

where d_{min} represents the minimum distance from the nearest-neighbour to the node.

These spatial characteristics influence which sites are most accessible and likely to receive or supply more material under different travel deterrence scenarios. To vary the network density and connectivity, a cut-off distance, d_δ, is applied to remove connections for which $d_{ij} > d_\delta$. The threshold may be defined using a selected δ^{th} percentile of all pairwise travel distances in d_{ij}. Increasing d_δ decreases network density and may lead to isolated nodes or disconnected clusters, thereby limiting feasible material transfers.

3 Results and Discussion

The results and discussion are organised into four scenarios derived from the analytical formulation of the network model to examine system behaviour and model viability under different constraints. The first scenario considers flow-constrained conditions in a homogeneous network with varying storage capacity, followed by geographically constrained conditions that assess the effect of distance cut-off thresholds on excess supply. The third scenario applies material-specific constraints to compare embodied carbon with transport-related emissions and determine storage requirements. The final scenario examines the distribution of storage capacity based on supply, demand and node centrality. The last two scenarios are presented using Great Britain as a case study, demonstrating how the spatial distribution of storage capacity affects network performance for a selection of reusable building materials using real transport distances from the national road network. The overall analysis evaluates storage requirements, the influence of process efficiencies ϕ and λ on material reuse, and the limits of transport distance beyond which reuse is no longer environmentally justified.

3.1 Flow and storage constraints

For a homogeneous network with uniform spatial distribution where all nodes are identical and equidistant from one another, $d_{ij} = 1$ for all nodes in a homogeneous network such that $i = j = n$, implying uniform accessibility throughout the network and d_{ij} can be omitted. For a network of size N, the storage level at time t for any node n ($s_{n,t}$) is determined by the relationships between total supply ($p_{n,t}$), total demand ($a_{n,t}$), maximum storage capacity ($c_{\max,n}$), as well as the material-specific yield factor (ϕ_M) and the retention factor (λ_n). Therefore, storage levels at any node can be expressed under four combinations of constraint conditions based on Eq. 13-14 for inflows and Eq. 16-17 for outflows:

$$s_{n,t} = \begin{cases} \phi_M w_{n,t}, & \text{if } \sum p_{n,t} \leq \sum (c_{\max,n} - \lambda_n s_{n,t-1}), \text{ and } \sum \lambda_n s_{n,t-1} \leq \sum a_{n,t} \\ \lambda_n s_{n,t-1} + \phi_M w_t - a_{n,t}, & \text{if } \sum p_{n,t} \leq \sum (c_{\max,n} - \lambda_n s_{n,t-1}), \text{ and } \sum \lambda_n s_{n,t-1} > \sum a_{n,t} \\ c_{\max,n} - \lambda_n s_{n,t-1}, & \text{if } \sum p_{n,t} > \sum (c_{\max,n} - \lambda_n s_{n,t-1}), \text{ and } \sum \lambda_n s_{n,t-1} \leq \sum a_{n,t} \\ c_{\max,n} - a_{n,t}, & \text{if } \sum p_{n,t} > \sum (c_{\max,n} - \lambda_n s_{n,t-1}), \text{ and } \sum \lambda_n s_{n,t-1} > \sum a_{n,t} \end{cases} \tag{21}$$

The four equations derived above provide a simplified analytical basis for understanding storage dynamics in a homogeneous network setting. For comparison to heterogeneous network scenarios, Monte-Carlo simulations were conducted and included in the sensitivity analysis attached in the Supplementary Information.

3.2 Hybrid demand- and supply-driven flow constraints

A novel contribution of this study is the development of the analytical formulation based on the conceptual framework illustrated in Figure 1 to capture the dynamical relationships of the gravity-based spatial interactions defined in Eq. 6-7. By treating supply and demand as independent variables, the model operates as a hybrid demand- and supply-driven mechanism. This allows the model to be constrained simultaneously by available supply, demand requirements, storage capacity, and temporal mismatches between inflow and outflow. The model captures the dynamic flow allocation between nodes in both storage-inflow and -outflow directions to track changes in storage levels, excess supply (ε_p) and excess demand (ε_a) over a time period T with a fixed time interval t, subject to the material yield factor (ϕ) and the storage retention factor (λ).

Figure 2 presents the results for a homogeneous network under different constraint conditions. The analysis includes randomly sampled values of ϕ and λ from a uniform distribution and varying number of nodes. The constraint condition is determined by the ratio of $\frac{c_{\max,n}}{w_{n,t}}$ where $w_{n,t}$ and $a_{n,t}$ are equal in these cases.

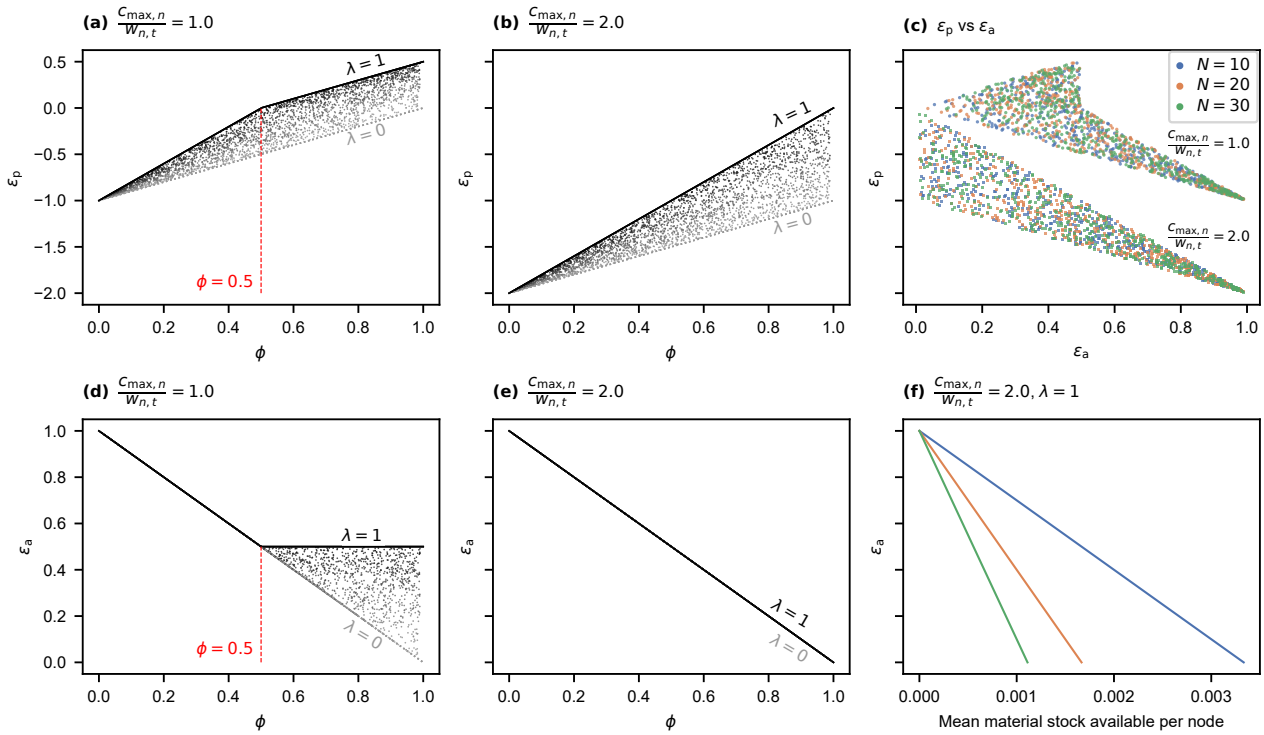


Figure 2: Excess supply (ε_p) and excess demand (ε_a) results against scattered random values of the material yield factor (ϕ) and the storage retention factor (λ) in a homogenous network, including the boundary value when $\lambda = 0$ (dashed-line) to $\lambda = 1$ (solid line). For varying constraint conditions, the total storage capacity, $c_{\max,n}$, is expressed as a ratio of $\frac{c_{\max,n}}{w_{n,t}} = 1.0$ in **(a)** and **(d)**, and $\frac{c_{\max,n}}{w_{n,t}} = 2.0$ in **(b)** and **(e)**, for fixed flows where $w_{n,t} = a_{n,t}$. In each of these cases, ε_p against ε_a results are also plotted in **(c)** to show that varying network size, N, has no direct impact on the results, with varying mean material stock available per node for each N in **(f)**.

The results show that variations in supply and demand resulted in distinctive flow scenarios and different storage utilisation patterns, even when storage capacity was assumed to be much larger than the total supply and demand. In some cases, equal supply and demand values may still resulted in under-utilisation of the storage space due to temporal mismatches between supply and demand, as storage became filled and can no longer accept new supply before material could be transferred out to meet demand. In contrast, under flow-constrained conditions, sufficient storage space may result in negative excess supply due to unused capacity and leading to higher operational costs. The distributions of ε_p against ε_a across different network sizes indicating that N has no direct effect on the results in a flow-constraint homogeneous network. In addition, behaviours of storage system under varying constraints generated from the numerical model built based on the analytical formulations in Eq. 21 are provided in the Supplementary Information.

To examine storage utilisation when the supply is limited by total waste availability, $\sum w_{i,t}$, two demand scenarios are considered to evaluate the requirements of $c_{max,n}$, under varying ϕ and λ factors. For a homogeneous network, and to avoid a capacity-constrained condition at inflow, setting $\varepsilon_{p,t}$ to zero from Eq. 15 gives:

$$c_{\max,n} = \phi_M w_{n,t} + \lambda_n \, s_{n,t-1} \tag{22}$$

For a high-demand scenario, a stock-constrained condition applies when $\sum \lambda_n s_{n,t-1} < \sum a_{n,t}$, assum-

ing $s_{n,t} = \phi_M w_t$ as all carried over stock material is fully absorbed at every t,:

$$c_{\max,n} = \phi_M(1 + \lambda_n)\, w_{n,t} \tag{23}$$

For a low-demand scenario, a demand-constrained scenario applies when $\sum \lambda_n s_{n,t-1} > \sum a_{n,t}$, assuming $s_{n,t} = c_{max,n}$ and all storage is fully occupied while demand approaches zero:

$$c_{\max,n} = \frac{\phi_M\, w_{n,t}}{(1 - \lambda_n)} \tag{24}$$

These show that, theoretically, in a flow-constrained scenario, assuming a homogeneous network with unlimited storage space and equidistance from all other nodes, maximum reuse (material savings) can be achieved by maximising the recovery efficiency ϕ_M to salvage as much reusable material as possible from recovered waste when the total availability of input supply flow is limited.

3.3 Heterogeneous network with geographical constraints

The assumption of a homogeneous network suggests that storage capacity requirements under different flow constraints are unaffected by network size when geographical constraints are not considered. In practice, however, travel deterrence is a crucial element of the spatial logistics of storage for CDW reuse. This section examines the influence of node locations and the distances between them in a heterogeneous network with geographical constraints, placed within a specified boundary. By varying N while keeping total supply, demand, and storage capacity constant, this analysis investigates the effects of distributing the same total storage capacity across either a large number of small storage sites or a small number of large storage sites within the same area.

In this analysis, for each N, the storage points are uniformly distributed from the center in a 'sunflower' shape across a fixed coverage area within a specific geographical boundary. Increasing N will bring the sites closer together and reduce the travel distances and the associated transport emissions. Using the pairwise distance d_{ij}, the flow allocation can be determined using the gravity-based formulation in Eq. 2. Travel deterrence is imposed by removing routes with distances greater than the cut-off distance, d_δ, defined at the δ^{th} percentile of all d_{ij} values in the distance adjacency matrix. Consequently, a lower threshold reduces the network density, which is defined as the proportion of remaining edges in relative to the total number of possible connections. Removing edges may lead to node isolation when all routes to a node are removed. Figure 3 shows the resulting changes in ε_p for $T = 10\Delta t$, the difference in spatial distance distribution, and the impact on network density with varying δ and N. Note that $\theta = 2$ is used throughout this analysis.

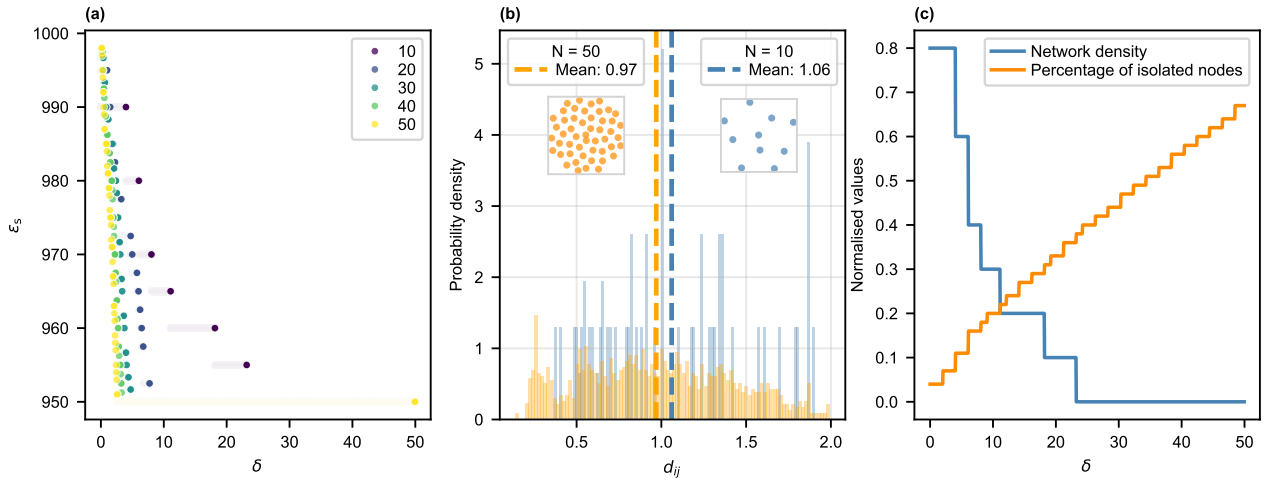


Figure 3: **(a)** Excess supply ε_p against the distance cut-off threshold (δ) for increasing network size (N) in a heterogeneous network covering the same area. **(b)** Change in probability density of pairwise distances (d_{ij}) and mean distances for a 'sunflower' network topology when N increases from 10 to 50. **(c)** Inverse relationship between network density and number of isolated nodes against δ for $N = 10$.

ε_p falls faster with δ in larger networks, exhibiting a steeper gradient where non-zero ε_p first appears at a lower threshold. This is because excess supply is primarily driven by the isolation of nodes once routes to the nearest-neighbour beyond the cut-off distance are removed at any node, preventing material from reaching other storage sites. This means that, under geographical constraints, spatial accessibility becomes a key limiting factor in CDW reuse, even when total network storage capacity is sufficient, and that nearest-neighbour distances can be used to define the minimum cut-off distance required in order to maintain feasible connections between nodes.

The analysis also examines how spatial distribution affects flow outcomes in alternative network topologies for $N = 100$. For larger networks, different topology arrangements, including a 'sunflower' network with nodes spreading radially from the centre with uniform spacing, a circular ring network with fixed radius, and a random network, produce different pairwise distance distribution. The resulting pattern of ε_p follows a similar general behaviour as the number of isolated nodes across these topologies, indicating that travel cut-offs and node isolation are the main drivers of excess supply. See the Supplementary Information for more details.

3.4 Maximum travel distance and storage capacity requirements under material constraints

This section examines the spatial requirements in terms of storage space and travel distance of specific materials using the national road-transport network of the Great Britain to present a real-world application. The analysis uses the centroids of all 350 local authorities as individual nodes. Weighted adjacency matrices are constructed from transport distances between centroids on the national road network, with routes restricted to HGV accessible roads, including major roads and motorways. Self-loop distances are also estimated as the shortest distance from each centroid to its nearest network boundary. The resulting distance distribution spans the national network, with the longest route approaching 1,302 km.

The flows of material are not only constrained by the availability of storage space and spatial accessi-

bility of the nodes, but also depend the types of material considering their embodied carbon emissions for potential carbon savings, comparing to the transport emissions. To justify the environmental benefits of material reuse, this study focuses on material mass and associated embodied carbon emissions to obtain a maximum travel distance such that transport emissions do not exceed the potential embodied carbon savings from reuse. Embodied carbon conversion factors of the materials are taken from the ICE database [38] while transport emissions are calculated using UK GHG conversion factors for typical UK diesel HGVs at given loading conditions [39]. As results, Figure 4 shows the maximum travel distance for a fixed load of precast concrete block, clay brick and timber, computed from their respective embodied carbon emissions and the indicative storage requirements for each material within the spatial range from the supply origin location.

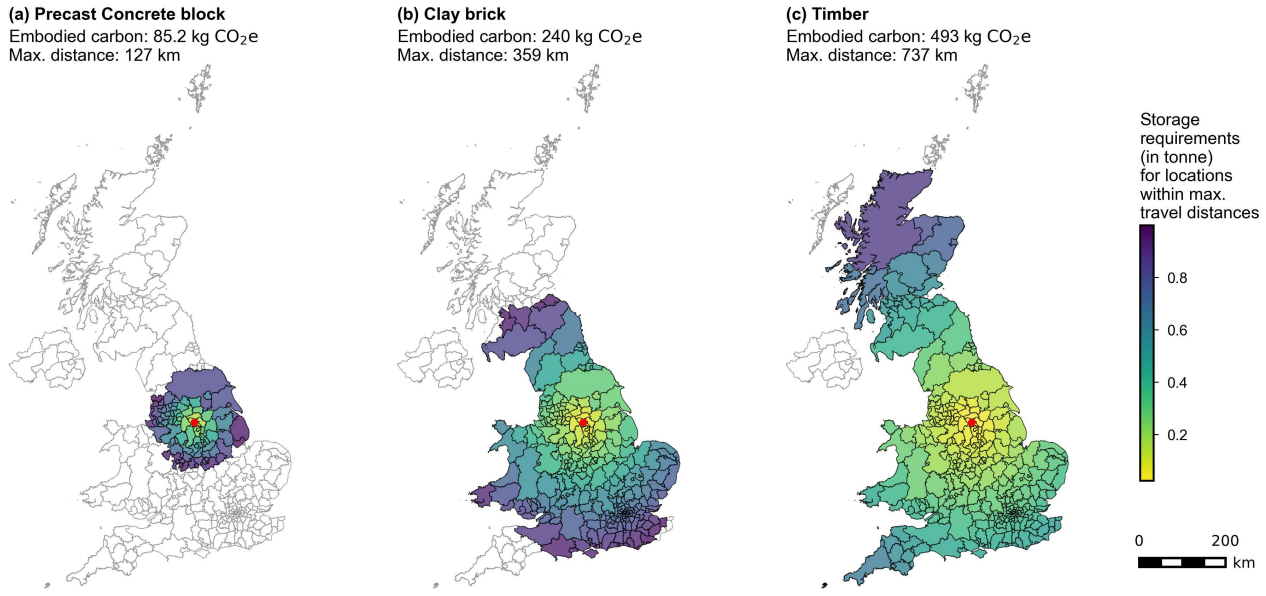


Figure 4: Map representations of Great Britain showing storage capacity requirements within the maximum travel distance per unit tonne of the following three construction materials, **(a)** precast concrete block, **(b)** clay brick and **(c)** timber, with the respective embodied carbon value for the material. Shaded areas indicate storage requirements in tonnes on a shared scale, the red marker identifies the origin location at Sheffield as reference.

Using Sheffield as the origin, three different materials are compared, each with a different travel range representing the maximum transport distance per tonne for which transport emissions remain justified by embodied carbon savings from a whole-life perspective. For example, precast concrete block has the smallest range, while clay brick can travel further due to its higher embodied carbon emissions per kilogram, and timber spans almost the entire map, with only a small number of nodes in the north falling outside the threshold, reflecting its substantially higher embodied carbon value. The shaded areas indicate the minimum material mass required to justify transport emissions, which also corresponds to the minimum storage capacity required at any location within the range. These results highlight the role of material-specific transport limitations and storage requirements in shaping the agglomeration of storage infrastructure sites. Materials with higher embodied carbon can be routed over longer distances and may justify larger, more centralised national facilities. Materials with lower embodied carbon require shorter transport distances to remain environmentally beneficial so smaller, locally distributed storage sites located near supply and demand nodes are more suitable.

Furthermore, the framework can be extended to consider other transport modes and their associated loading constraints, such as vehicle weight and size limits. For construction materials, additional functional units, such as geometric volume or packing volume, can be incorporated to account for bulky materials that require special handling. To compare transport emissions with embodied carbon emissions across different types of material, the framework estimates the maximum transport distance for each material given its embodied carbon value, with the option to vary loading conditions and transport modes. For a fully-loaded vehicle, the maximum distance is limited by the legal maximum load for that vehicle type. For alternative applications, if the origin and destination locations are fixed, the framework can be used to estimate the minimum quantity of material required to justify transport emissions over longer distances. See Supplementary Information for additional details.

3.5 Distribution of maximum storage capacity

Finally, this study examines how the spatial distribution of storage capacity affects material-throughput and the resulting ε_p under different scaling factors. The maximum storage capacity at a node, $c_{\max,i}$, is scaled with the distribution of material supply and demand, and the closeness-centrality of each node based on its geographical location. For the supply and demand distributions, the number of new homes and demolitions from the annual housing statistics at the local authority level are used as proxies for material supply and demand [40–42], while keeping the national totals unchanged and remain constant over time. In network analysis, closeness-centrality is defined as the reciprocal of the average shortest-path distance from a node to all other connected nodes such that higher centrality means higher importance and greater potential to distribute more efficiently [43].

Figure 5 shows the spatial distributions of $c_{\max,i}$ when scaled with the material supply, demand and closeness-centrality of each local authority, with ϕ_M and λ_i are fixed to 1. All values are normalised to show the percentages.

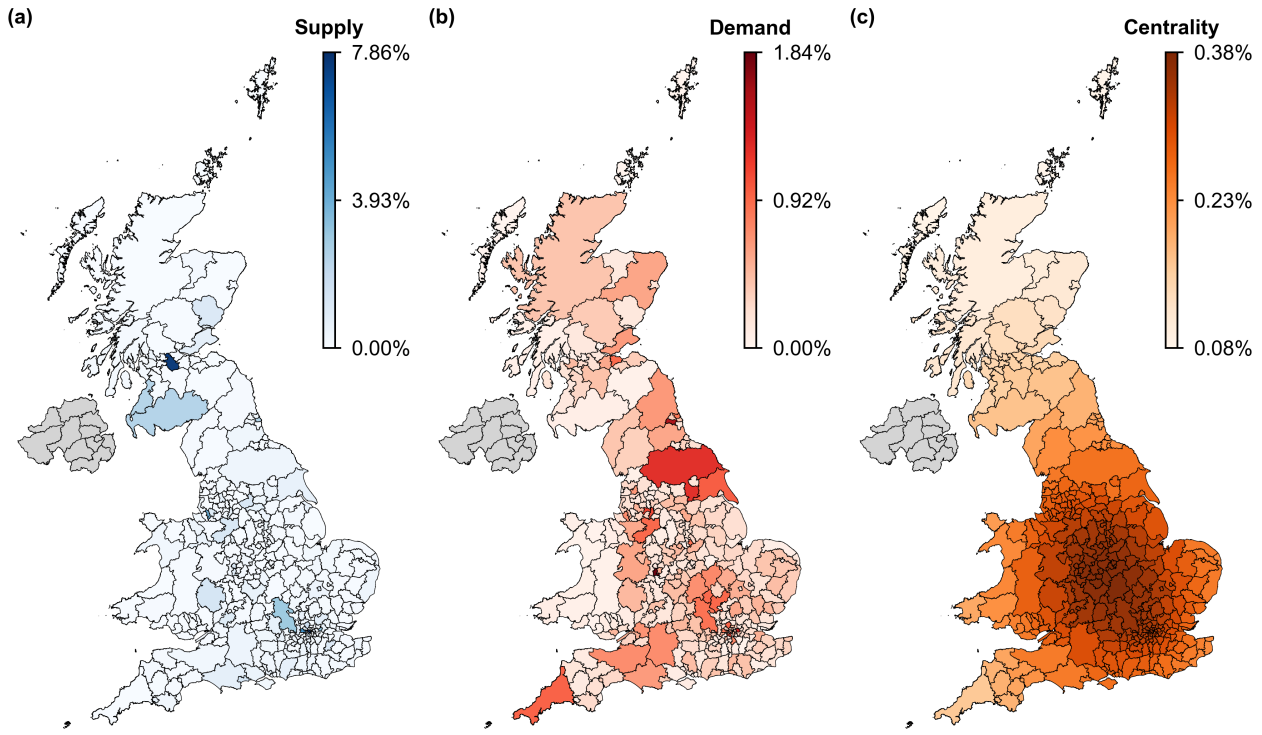


Figure 5: Spatial distributions of the $c_{\max,i}$ under scaling by **(a)** material supply, **(b)** material demand, and **(c)** the closeness-centrality, for each local authority in the Great Britain. Values are normalised to show the percentages.

Next, by imposing travel deterrence on the network, Figure 6 shows the corresponding material-throughput in inflow and outflow directions, denoted by T_{in} and T_{out} respectively, and the results of ε_p and ε_a, plotted against the distance cut-off threshold δ for each scaling factor.

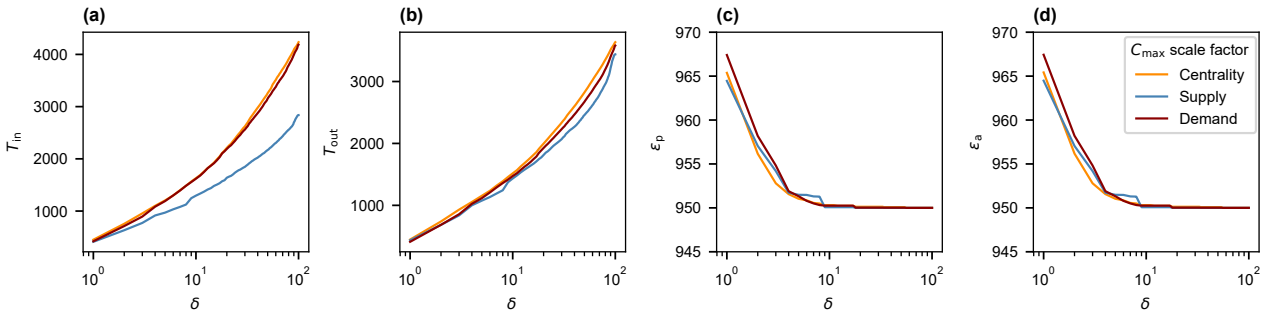


Figure 6: Results of material-throughput for **(a)** storage-inflows (T_{in}), **(b)** storage-outflows (T_{out}), **(c)** Excess Supply (ε_p), and **(d)** Excess Demand (ε_a), against the distance cut-off threshold (δ) for each scaling factor.

The results show broadly similar patterns in excess supply and demand across the different scaling strategies as the total quantity of material in the system remains unchanged with no material loss, but different ways of distributing it spatially. Differences are more apparent in the material-throughput for storage-inflows. When storage capacity is scaled by supply, inflow-throughput to storage is lower than under the others, indicating that more material is stored closer to the supply source and travels shorter distances. This suggests that allocating more storage space within the same, or close to, the

supply nodes can reduce transport loads and associated emissions. As such, these findings can inform decision makers on where resources should be invested when total storage capacity is fixed on the system-level, as the maximum storage capacity should be allocated not only on the basis of embodied carbon and transport limits, but also in relative to the spatial distribution of supply and demand.

3.6 Limitations and Future work

There are several limitations in this work that may suggest directions for future work.

1. The analysis currently considers only one transport mode and assumes conventional HGV operations. Future work could include alternative low-carbon transport options, as well as policy-imposed limits on transport distances and carbon emissions of CDW.

2. Material flows are currently represented in terms of aggregated mass and their associated embodied carbon. Incorporating more detailed information on material specifications and component-level characteristics would improve estimates of recoverability and provide more accurate assessments of the volumetric requirements for transport loads and storage space, supporting more realistic applications.

3. Effective reuse of CDW material is likely to be influenced by industry practices and policy regulations such as recovery pathways, waste classification standards and procurement requirements. The framework could consider these external conditions to reflect real-world constraints.

4 Conclusion

This study introduces a novel spatial gravity framework for optimising storage capacity and its distribution to facilitate material reuse in the built environment. The framework accounts for dynamic supply and demand in material flows, and explicitly incorporates constraints arising from storage capacity, geographical location, travel deterrence, and material-specific requirements. This provides a new conceptual and methodological basis for understanding the spatial requirements of storage infrastructure and the distribution of storage capacity across regional and national transport and logistic networks.

The analysis yields four key findings. First, under flow-constrained conditions in a homogeneous network with unlimited storage and equidistant nodes, maximum reuse is achieved by maximising recovery efficiency when input supply is limited. Second, under geographical constraints, travel deterrence can cause excess supply or excess demand even when aggregate storage capacity is sufficient, because node isolation restricts spatial accessibility to feasible storage locations. Third, material-specific transport and storage requirements determine whether reuse is better supported by centralised or distributed storage infrastructure for which materials with higher embodied carbon can justify longer travel distances and more centralised facilities, whereas materials with lower embodied carbon require shorter distances and are better suited to locally distributed storage. Fourth, the maximum storage capacity should be allocated in relation to both embodied carbon and the spatial distribution of supply and demand, while scaling storage capacity towards supply nodes reduces transport distances and associated emissions.

For implications of this study, the framework can help decision-makers identify where to invest in storage infrastructure when total capacity is fixed, and can be used to determine the spatial agglom-

eration of more centralised or distributed storage under different material and transport limitations. It also offers a way to link storage planning with wider circular economy goals such as CDW waste recovery efficiencies, transport decarbonisation and local development targets.

Data availability statement

All additional information and data generated in this study are included in the Supplementary Information (SI) provided. SI1 provides the additional details of the findings discussed in the results; SI2 contains the validation data generated from the Monte-Carlo simulations with varying size N; SI3 contains the GB case study data.

Author contributions

All authors contributed to the study conception and design. Ling Min Tan developed the methodology, performed data acquisition and analysis, wrote the first draft and revised the manuscript. Hadi Arbabi validated the method, reviewed and commented on the manuscript. All authors read and approved the final manuscript.

Acknowledgments

This work was supported by UKRI EPSRC funding EP/Y530578/1.

References

[1] United Nations Environment Programme. Building materials and the climate: Constructing a new future. Report, UN Environment Programme, 2024. URL https://www.unep.org/resources/report/building-materials-and-climate-constructing-new-futu

[2] Liyin Shen, Vivian W. Y. Tam, C. M. Tam, and Derek S. Drew. Mapping approach for examining waste management on construction sites. *Journal of Construction Engineering and Management*, 130(4):472–481, August 2004. doi: 10.1061/(ASCE)0733-9364(2004)130:4(472).

[3] Haiming Lyu, Bo Xiong, et al. Estimation of construction and demolition waste and assessment of disposal facility location: An integrated Material Flow Analysis and Geographic Information System approach. *Resources, Conservation and Recycling*, 217:108226, May 2025. doi: 10.1016/j.resconrec.2025.108226.

[4] Sourabh Jain, Shaleen Singhal, and Nikunj Kumar Jain. Construction and demolition waste generation in cities in India: an integrated approach. *International Journal of Sustainable Engineering*, 12(5):333–340, May 2019. doi: 10.1080/19397038.2019.1612967.

[5] European Parliament and Council. Directive 2008/98/ec... on waste. *Official Journal of the European Union*, L 312:3–30, 2008.

[6] United States Environmental Protection Agency. Sustainable management of construction and demolition materials, 2025. URL https://www.epa.gov/smm/sustainable-management-construction-and-demolition-materials. Accessed 13 October 2026.

[7] Kambiz Rakhshan, Jean-Claude Morel, Hafiz Alaka, and Rabia Charef. Components reuse in the building sector – a systematic review. *Waste Management & Research*, 38(4):347–370, 2020. doi: 10.1177/0734242X20910463.

[8] [Co-authors to verify] Sakthibala. A critical review on recycling and reuse of construction and demolition waste materials. *Cleaner Waste Systems*, page 100375, 2025. doi: 10.1016/j.clwas.2025.100375.

[9] Maria Menegaki and Dimitrios Damigos. A review on current situation and challenges of construction and demolition waste management. *Current Opinion in Green and Sustainable Chemistry*, 13:8–15, October 2018. doi: 10.1016/j.cogsc.2018.02.010.

[10] Shuai Zhu and Hui Feng. Construction and demolition waste circulation and its sustainability performance in the building sector: current trend and future directions. *Engineering, Construction and Architectural Management*, 33(5):4119–4148, 2026. doi: 10.1108/ECAM-05-2024-0678.

[11] Irene Papamichael, Ioanna Voukkali, Pantelitsa Loizia, and Antonis A. Zorpas. Construction and demolition waste framework of circular economy: A mini review. *Waste Management & Research*, 41(12):1728–1740, December 2023. doi: 10.1177/0734242X231195875.

[12] Dongchen Han, Mohsen Kalantari, and Abbas Rajabifard. The development of an integrated BIM-based visual demolition waste management planning system for sustainability-oriented decision-making. *Journal of Environmental Management*, 351:119856, February 2024. doi: 10.1016/j.jenvman.2023.119856.

[13] Zezhou Wu, Tianjia Pei, Zhikang Bao, S. Thomas Ng, Guoyang Lu, and Ke Chen. Utilizing intelligent technologies in construction and demolition waste management: From a systematic review to an implementation framework. *Frontiers of Engineering Management*, 12(1):1–23, 2025. doi: 10.1007/s42524-024-0144-4.

[14] Jaime A. Mesa, Carlos Fúquene-Retamoso, and Aníbal Maury-Ramírez. Life cycle assessment on construction and demolition waste: A systematic literature review. *Sustainability*, 13(14):7676, July 2021. doi: 10.3390/su13147676.

[15] Daina Kleponė and Kristina Kovaitė. What drives high-value construction and demolition waste recycling in the EU? *Waste Management Bulletin*, 5:100303, June 2026. doi: 10.1016/j.wmb.2026.100303.

[16] Michael Sansom and Nicholas Avery. Briefing: Reuse and recycling rates of UK steel demolition arisings. *Proceedings of the Institution of Civil Engineers – Engineering Sustainability*, 167(3): 89–94, June 2014. doi: 10.1680/ensu.13.00026.

[17] Interreg North-West Europe FCRBE. A guide for identifying the reuse potential of construction products. Project guidance, Interreg North-West Europe / Rotor DB, 2021. URL `https://rotordb.org/en/projects/interreg-nwe-fcrbe`. Accessed 13 October 2026.

[18] Federal Office for the Environment (FOEN). Circular economy country profile: Switzerland. Country profile, European Environment Information and Observation Network (Eionet) / Swiss Federal Office for the Environment, 2024. URL `https://www.eea.europa.eu/en/topics/in-depth/circular-economy/country-profiles-on-circular` $country - profile_final.pdf. Accessed 13 October 2026.$

[19] Keilla R. A. Nunes, Cláudio F. Mahler, and Raquel Valle. Reverse logistics in the Brazilian construction industry. *Journal of Environmental Management*, 90(12):3717–3720, September 2009. doi: 10.1016/j.jenvman.2008.05.026.

[20] Gihan Anuradha Tennakoon, Raufdeen Rameezdeen, and Nicholas Chileshe. Identifying factors affecting the low uptake of reprocessed construction materials: A systematic literature review. *Waste Management & Research*, 41(4):781–800, April 2023. doi: 10.1177/0734242X221135244.

[21] Dimitris Aidonis, Eleftherios Iakovou, Dimitrios Vlachos, and Alexandros Xanthopoulos. An analytical methodological framework for managing reverse supply chains in the construction industry. *CIRP Journal of Manufacturing Science and Technology*, 1(2):91–105, 2008. doi: 10.1016/j.cirpj.2008.09.005.

[22] Verena Göswein, Ana Bras Gonçalves, José D. Silvestre, Fausto Freire, Guillaume Habert, and Rashad Kurda. Transportation matters–does it? GIS-based comparative environmental assessment of concrete mixes with cement, fly ash, natural and recycled aggregates. *Resources, Conservation and Recycling*, 137:1–10, October 2018. doi: 10.1016/j.resconrec.2018.05.028.

[23] Eleni Iacovidou and Phil Purnell. Mining the physical infrastructure: Opportunities, barriers and interventions in promoting structural components reuse. *Science of the Total Environment*, 557–558:791–807, July 2016. doi: 10.1016/j.scitotenv.2016.03.098.

[24] Lu Ding, Tong Wang, and Paul W. Chan. Forward and reverse logistics for circular economy in construction: A systematic literature review. *Journal of Cleaner Production*, 388:135981, February 2023. doi: 10.1016/j.jclepro.2023.135981.

[25] Toby Tsui, Alexis Derumigny, Dick Peck, Arjan van Timmeren, and Alexander Wandl. Spatial clustering of waste reuse in a circular economy: A spatial autocorrelation analysis on locations of waste reuse in the Netherlands using global and local Moran's I. *Frontiers in Built Environment*, 8:954642, August 2022. doi: 10.3389/fbuil.2022.954642.

[26] Xining Yang, Mingming Hu, Wenhui Shan, Chunbo Zhang, Tiankun Li, and Yingji Pan. Integrating bottom-up building stock model with logistics networks to support the site selection of circular construction hub. *Journal of Cleaner Production*, 429:139479, December 2023. doi: 10.1016/j.jclepro.2023.139479.

[27] Gang Cai and Dietmar Waldmann. A material and component bank to facilitate material recycling and component reuse for a sustainable construction: concept and preliminary study. *Clean Technologies and Environmental Policy*, 21:2015–2032, 2019. doi: 10.1007/s10098-019-01758-1.

[28] Marie Vejlin Buchard and Thomas Budde Christensen. Business models for the reuse of construction and demolition waste. *Waste Management & Research*, 42(5):359–371, May 2024. doi: 10.1177/0734242X231188023.

[29] J. Nicolas and B. Sébastien. Barriers to reuse in the construction sector: A circular value chain perspective. *Business Strategy and the Environment*, pages 1–18, 2026. doi: 10.1002/bse.70549.

[30] United Nations Environment Programme. Global status report for buildings and construction 2024/2025. Report, UN Environment Programme, 2025. URL `https://www.unep.org/resources/report/global-status-report-buildings-and-construction`.

[31] Rayra Brandão, David John Edwards, Mohammad Reza Hosseini, André Cristiano Silva Melo, and Alcebíades Negrão Macêdo. Reverse supply chain conceptual model for construction and demolition waste. *Waste Management & Research*, 39(11):1341–1355, 2021. doi: 10.1177/0734242X211008778.

[32] Jean-Paul Rodrigue. *The Geography of Transport Systems*. Routledge, 5th edition, 2020. URL https://transportgeography.org/contents/methods/spatial-interactions-gravity-model/.

[33] Yu Liu, Shengyin Wang, Xuechen Wang, Yunhao Zheng, Xinyan Chen, and Yuhao Kang. Towards semantic enrichment for spatial interactions. *Annals of GIS*, 30(2):151–166, April 2024. doi: 10.1080/19475683.2024.2324392.

[34] James E. Anderson. A theoretical foundation for the gravity equation. *American Economic Review*, 69(1):106–116, March 1979. URL https://www.jstor.org/stable/1802501. First theoretical foundation for the gravity equation.

[35] Juan Caballero Reina, Jesús Crespo Cuaresma, Katharina Fenz, Jakob Zellmann, Teodor Yankov, and Amr Taha. Gravity models for global migration flows: A predictive evaluation. *Population Research and Policy Review*, 43(2):29, April 2024. doi: 10.1007/s11113-024-09867-6.

[36] William Alonso. A theory of movements. In Niles M. Hansen, editor, *Human Settlement Systems: International Perspectives on Structure, Change and Public Policy*, pages 197–211. Ballinger Publishing Company, Cambridge, Massachusetts, 1978.

[37] Jacob J. de Vries, Peter Nijkamp, and Piet Rietveld. Alonso's general theory of movement: Advances in spatial interaction modeling. Tinbergen Institute Discussion Paper 00-062/3, Tinbergen Institute, Amsterdam and Rotterdam, May 2000. URL https://ideas.repec.org/p/tin/wpaper/20000062.html.

[38] Circular Ecology. Inventory of carbon and energy (ICE) database [version 4.1]. Circular Ecology, 2025. URL https://circularecology.com/embodied-carbon-footprint-database.html. Accessed 13 October 2026.

[39] Department for Energy Security and Net Zero. 2026 government greenhouse gas conversion factors for company reporting: Methodology paper and data tables. Government publication, Department for Energy Security and Net Zero, June 2026. URL https://www.gov.uk/government/publications/greenhouse-gas-reporting-conversion-factors-202 Published 11 June 2026; accessed 13 October 2026.

[40] Ministry of Housing, Communities and Local Government. Housing supply: Net additional dwellings, england: 2024 to 2025. Accredited official statistics, Ministry of Housing, Communities and Local Government, November 2025. URL https://www.gov.uk/government/statistics/housing-supply-net-additional-dwellings-england-2 Published 20 November 2025; accessed 13 October 2026.

[41] Welsh Government. Housing. StatsWales, 2026. URL https://stats.gov.wales/en-GB/topic/56/housing. Accessed 13 October 2026.

[42] Scottish Government. Housing statistics for scotland: New housebuilding. Scottish Government, 2026. URL https://www.gov.scot/publications/housing-statistics-for-scotland-new-house-build Quarterly housing statistics update; published 29 September 2026; accessed 13 October 2026.

[43] Gert Sabidussi. The centrality index of a graph. *Psychometrika*, 31(4):581–603, December 1966. doi: 10.1007/BF02289527. Defined the standard distance-based centrality formulation in graph theory.

Supplementary Files

This is a list of supplementary files associated with this preprint. Click to download.

- SupplementaryInformationSI1figures.pdf
- SupplementaryInformationSI3.2GBdemand.csv
- SupplementaryInformationSI3.3GBsupply.csv
- SupplementaryInformationSI3.1GBcentrality.csv
- SupplementaryInformationSI2.1MCN10.csv
- SupplementaryInformationSI2.3MCN1000.csv
- SupplementaryInformationSI2.2MCN100.csv